Dalton Transactions

ROYAL SOCIETY OF CHEMISTRY

PAPER

View Article Online
View Journal | View Issue

Open Access Article. Published on 10 September 2024. Downloaded on 6/5/2026 2:59:47 PM.
This article is licensed under a Creative Commons Attribution-NonCommercial 3.0 Unported Licence.

Check for updates

Cite this: *Dalton Trans.*, 2024, **53**, 16202

A new family of heterometallic [Cu_6M_4] (M = Gd, Tb, Dy and Y) clusters derived from the combined use of selected pyridyl poly-alcohol ligands†

Antonis Anastassiades,[a] Dimitris I. Alexandropoulos, ‡[a] Christian D. Buch,[b] Stergios Piligkos *[b] and Anastasios J. Tasiopoulos *[a]

Received 16th July 2024,
Accepted 4th September 2024

DOI: 10.1039/d4dt02054e

rsc.li/dalton

The combined use of 2-(2-pyridyl)-1,3-propane-diol ($pypdH_2$) and 2-hydroxymethyl-2-(2-pyridyl)-1,3-propane-diol ($pyptH_3$) in Cu^{2+}/4f chemistry has afforded a new family of isostructural [$Cu_6M_4(pypt)_4(pypdH)_4(NO_3)_8$] [M = Gd (**1**), Tb (**2**), Dy (**3**), and Y (**4**)] complexes. These compounds are based on an unprecedented three-layered symmetric [$Cu_6M_4(\mu\text{-}OR)_{16}]^{8+}$ structural core, formed from the connection of the metal ions by bridging alkoxide arms of the organic ligands. Direct current magnetic susceptibility studies for complexes **1–3** revealed the presence of dominant ferromagnetic exchange interactions, suggesting the existence of large spin ground state values. Alternating current magnetic studies indicate the presence of slow-magnetic relaxation in **1–3**.

Introduction

Heterometallic Cu^{2+}/Ln^{3+} complexes represent a fascinating frontier in the field of coordination chemistry. The interest is driven by the potential of these molecules to exhibit unprecedented structural motifs and intriguing electronic and magnetic properties.[1–3] The growth of this area is largely attributed to two major discoveries that took place a long time ago: the observation of ferromagnetic Cu^{2+}/Gd^{3+} coupling in a {Cu_2Gd} complex in 1986,[4] and the detection of single-molecule magnetism behaviour (SMM) in a {Cu_2Tb_2} compound in 2004.[5] Since then, tremendous effort has been put into the synthesis of Cu^{2+}/Ln^{3+} complexes and research in this field has afforded many beautiful coordination complexes with large nuclearities[6–9] and aesthetically pleasing structural motifs not found in homometallic 3d- or 4f-metal clusters.[10–14] This structural variability of Cu^{2+}/Ln^{3+} complexes arises from the versatile coordination geometries of Cu^{2+} and Ln^{3+} ions.

The interest of Cu^{2+}/Ln^{3+} complexes in the field of molecular magnetism is mainly focused in the areas of single molecule magnets[15–17] and molecular magnetic refrigerants.[18,19] The intrinsic characteristics of lanthanide ions and particularly their unquenched orbital angular momenta and the presence of numerous unpaired electrons, endow these ions with significant magnetic moments and anisotropy.[20–23] However, polymetallic lanthanide complexes display very weak intramolecular exchange interactions, leading to fast magnetic relaxation through quantum tunnelling of magnetization (QTM).[24] One method that has been employed to afford 4f-containing clusters with stronger magnetic interactions as compared to these of purely 4f systems involves the incorporation of 3d metal ions into these systems. This method also allows the mitigation of QTM and, in the case of ferromagnetic interactions,[25–28] the formation of systems with large spin ground states.[29] Among the various families of 3d/4f metal clusters, Cu^{2+}/4f compounds have attracted significant attention because of the strong and often ferromagnetic (*vide supra*) exchange interactions of Cu^{2+} and Ln^{3+} ions. Thus, complexes containing highly anisotropic lanthanide ions like Dy^{3+} along with Cu^{2+} ions, can meet the requirements of single-molecule magnets (SMMs) and exhibit slow magnetization relaxation,[30–34] whereas complexes consisting of isotropic Gd^{3+} ions (and Cu^{2+} ions) are good candidates to exhibit enhanced magnetocaloric effect (MCE) and act as molecular magnetic refrigerants.[17,35–39]

The synthesis of Cu^{2+}/4f clusters depends on numerous synthetic parameters, one of which is the choice of the organic ligand. In fact various organic ligands containing either O or O/N donor atoms have been employed in the synthesis of Cu^{2+}/4f clusters including polydentate Schiff bases,[1,40,41] oximes,[38,42,43] alcohols,[35,44–47] and amino acids.[48–50] Given

[a]*Department of Chemistry, University of Cyprus, 1678 Nicosia, Cyprus. E-mail: atasio@ucy.ac.cy*

[b]*Department of Chemistry, University of Copenhagen, DK-2100, Denmark*

†Electronic supplementary information (ESI) available: Various structural tables, spectroscopic and magnetic figures and tables for complexes **1–4**. CCDC 2370731–2370734. For ESI and crystallographic data in CIF or other electronic format see DOI: https://doi.org/10.1039/d4dt02054e

‡Current Address: Department of Chemistry, University of Patras, 26504 Patras, Greece.

This journal is © The Royal Society of Chemistry 2024

Open Access Article. Published on 10 September 2024. Downloaded on 6/5/2026 2:59:47 PM. This article is licensed under a Creative Commons Attribution-NonCommercial 3.0 Unported Licence.

that alcohol containing ligands have afforded Cu^{2+}/4f clusters with aesthetically pleasing structures[11,33,35,44–47] and based on our experience in the mixed-ligand approach,[51] we investigated reactions that included the combined use of 2-(2-pyridyl)-1,3-propane-diol ($pypdH_2$) and 2-hydroxymethyl-2-(2-pyridyl)-1,3-propane-diol ($pyptH_3$) in Cu^{2+}/4f cluster chemistry (Scheme 1). These are flexible ligands, containing one aromatic N-donor atom and two ($pypdH_2$), or three ($pyptH_3$) aliphatic alcohol O atoms that can bind to various metal ions in many coordination modes, depending on the deprotonation level. Moreover, the versatility of the aliphatic alcohol oxygen atoms of these ligands enables them to accommodate metal ions across a wide range of ionic radii.[52] To the best of our knowledge, these ligands are employed for the first time in coordination chemistry although there are very few manganese and copper metal complexes, bearing the methyl substituted analogue of $pypdH_2$ ligand (2-methyl-2-(2-pyridyl)-1,3-propan-diol) (Table S5†).[53,54]

We report the syntheses, structures and magnetic properties of a new family of Cu^{2+}/4f clusters with the formula $[Cu_6M_4(pypt)_4(pypdH)_4(NO_3)_8]$ [M = Gd (**1**), Tb (**2**), Dy (**3**), and Y (**4**)]. They are the first examples of coordination complexes containing the ligands $pypdH_2$ and $pyptH_3$ and display an unprecedented three-layered symmetric $[Cu_6M_4(\mu\text{-}OR)_{16}]^{8+}$ structural core. Direct current (dc) and alternating current (ac) magnetic susceptibility studies suggest the presence of dominant ferromagnetic exchange interactions and of slow relaxation of the magnetization process for compounds **1–3**.

Results and discussion

Synthetic comments

Our group as well as other ones have a continuing interest on the use of polyol-type ligands in 3d and 3d/4f metal cluster chemistry.[55–58] Indeed, the use of such ligands in both homometallic Mn and heterometallic Mn/4f cluster chemistry either as primary organic chelating ligands[52,59,60] or in combination with various phenolic oximes[61–63] or $(py)_2CO$ derivatives,[64–67] yielded high nuclearity complexes with aesthetically pleasing structures and intriguing magnetic properties. An extension of these studies involves the use of $pypdH_2$ and $pyptH_3$ ligands, which bear resemblance to well-known polyol-type ligands including 1,3-propanediol (pdH_2) and 1,1,1-tris(hydroxymethyl)ethane ($thmeH_3$), respectively. These ligands were employed in 3d/4f cluster chemistry either as the main chelate or in combination with other chelates and we herein report the initial results of these efforts; a new family of Cu^{2+}/4f compounds obtained from the combined use of $pypdH_2$ and $pyptH_3$.

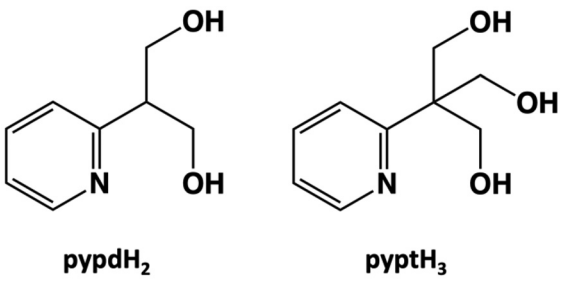

Scheme 1 Structural formulae and abbreviations of the ligands used in this work.

The general reaction of $Cu(NO_3)_2{\cdot}5/2H_2O$, $M(NO_3)_3{\cdot}xH_2O$ (M = Gd, Tb, Dy and Y), $pypdH_2$ and $pyptH_3$ in the presence of NEt_3 in a molar ratio of ~1 : 1 : 1 : 1 : 2.5 in MeCN resulted in a blue solution that was left undisturbed at room temperature to afford, after 1 day, blue crystals of **1–4** in high yields (~45–65%). The isolation of complexes **1–4** required the use of base. In fact, their isolation was independent of the organic/inorganic base that was used in the reaction mixture since they were isolated when Me_4NOH, $Bu^t{}_4NOH$, NaOH or Et_3N was used although the latter led to significantly higher reaction yield. In addition, the use of MeCN solvent, was essential for the isolation of **1–4** since the same reaction in other solvents (*i.e.*, MeOH, EtOH, DMF, CH_2Cl_2) led to microcrystalline or amorphous solids that could not be further characterized. Furthermore, the presence of NO_3^- anions from both Cu^{2+} and M^{3+} starting materials is crucial for the synthesis of **1–4**, since analogous reactions with different anions (*i.e.*, Cl^-, ClO_4^- and $MeCO_2^-$) led to insoluble precipitates which we were unable to crystallize. Finally, the presence of both organic ligands in the reaction mixture was essential for the isolation of **1–4**. The role of the two ligands, $pypdH_2$ and $pyptH_3$, was scrutinized through various modifications of the original synthetic procedure. The aim was to investigate whether analogous complexes containing only one of these ligands could be formed. However, these experiments did not result in the formation of crystalline materials. The formation of compounds **1–4** is summarized in eqn (1), where x = 5 or 6:

$$\begin{aligned} &6Cu(NO_3)_2\cdot 5/2H_2O + 4M(NO_3)_3\cdot xH_2O \\ &\quad + 4pypdH_2 + 4pyptH_3 + \\ &\quad 16Et_3N \xrightarrow{MeCN} [Cu_6M_4(pypt)_4(pypdH)_4(NO_3)_8] \\ &\quad + 16(Et_3NH)(NO_3) + (15+4x)H_2O \end{aligned} \quad (1)$$

The reported compounds were characterized by single-crystal X-ray crystallography, powder diffraction, elemental analyses (C, H, N), thermogravimetric analysis and IR spectroscopy. Details on the IR, pXRD and TGA studies for complexes **1–4** are available in ESI (Fig. S1–S3 and Table S6†). The protonation levels of the O atoms of $pypdH_2$ and $pyptH_3$ ligands were determined by charge-balance considerations, inspection of the metric parameters and BVS calculations (Table S3†).[68,69]

Description of structures

Compounds **1**·3MeCN, **2**·3MeCN, **3**·4MeCN and **4**·4MeCN are isostructural with their main difference being the lanthanide ions they contain and the number of lattice MeCN molecules. For this reason, only the structure of **1**·3MeCN will be described in detail as a representative example. Partially labelled representations of the structure of **1**·3MeCN are

Open Access Article. Published on 10 September 2024. Downloaded on 6/5/2026 2:59:47 PM.
This article is licensed under a Creative Commons Attribution-NonCommercial 3.0 Unported Licence.

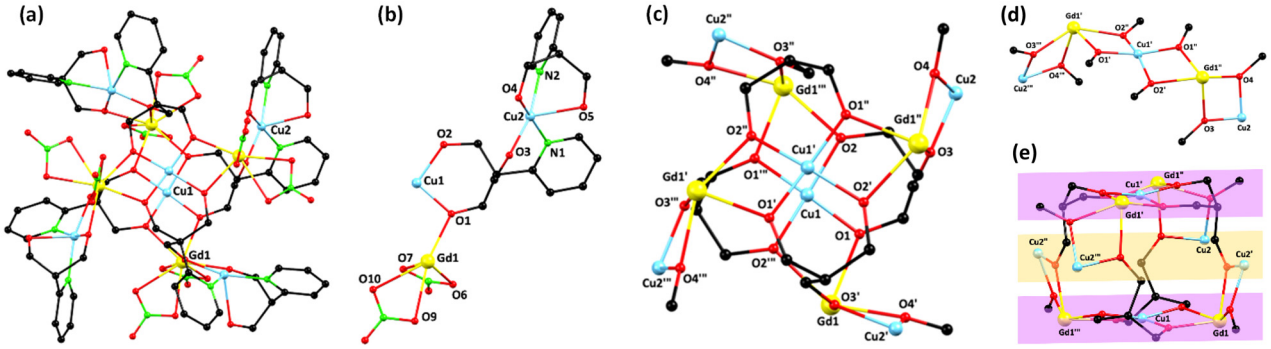

Fig. 1 Partially labelled representations of: (a) the molecular structure, (b) the asymmetric unit, (c) the metal/O core, (d) the pentanuclear $[Cu_3Gd_2(\mu\text{-}OR)_8]^{4+}$ sub-unit of the core and (e) the three-layered structure of **1**·3MeCN. H atoms and MeCN solvent molecules are omitted for clarity. Colour code: Cu^{2+}, cyan; Gd^{3+}, yellow; N, green; O, red; C, black. Symmetry codes: (′) $+x$, $1-y$, $1-z$, (″) $1-x$, $+y$, $1-z$, (‴), $1-x$, $1-y$, $+z$.

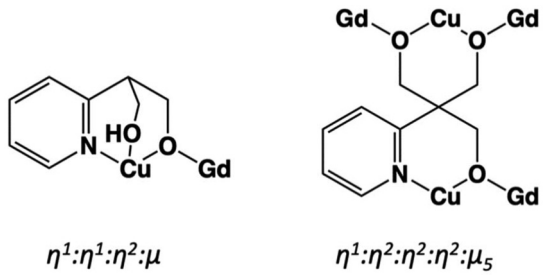

Scheme 2 Crystallographically established coordination modes of $pypdH^-$ and $pypt^{3-}$ ligands in complex **1**·3MeCN.

shown in Fig. 1. The coordination modes of the ligands $pypdH^-$ and $pypt^{3-}$ are illustrated in Scheme 2. Selected interatomic distances (Å) and angles (°) for **1**·3MeCN, **2**·3MeCN, **3**·4MeCN and **4**·4MeCN are shown in Table S4.† Complex **1**·3MeCN (Fig. 1a) crystallizes in the tetragonal space group $P\bar{4}2_1c$, with the asymmetric unit (Fig. 1b) featuring 1/4 of the neutral compound $[Cu_6Gd_4(pypt)_4(pypdH)_4(NO_3)_8]$. The compound consists of six Cu^{2+} and four Gd^{3+} ions bridged through the alkoxido arms of four singly deprotonated $pypdH^-$ and four triply deprotonated $pypt^{3-}$ ligands, possessing a symmetric $[Cu_6Gd_4(\mu\text{-}OR)_{16}]^{8+}$ metal core (Fig. 1c). The core of **1** displays a three-layered structure consisting of two equivalent $[Cu_3Gd_2(\mu\text{-}OR)_8]^{4+}$ units (Fig. 1d) that are held together by the four $pypt^{3-}$ ligands. The upper and lower layers comprise linear {GdCuGd} sub-units displaying different orientations and are separated by a central $\{Cu_4\}$ rectangle. Each pentametallic $[Cu_3Gd_2(\mu\text{-}OR)_8]^{4+}$ unit features an alternating Cu/Gd chain, where the three central metal ions, two Gd^{3+} ions and one Cu^{2+} ion, are arranged in an almost linear configuration. The remaining two Cu^{2+} ions are positioned 3.321 Å away from and on the same side of the plane formed by the metal ions of the linear {GdCuGd} sub-unit. The four Cu2 centers are located on the same plane, forming a rectangle, separating the two linear {GdCuGd} sub-units and giving rise to the three-layered structure of **1** (Fig. 1d). The four singly-deprotonated $pypdH^-$ ligands bridge a Cu^{2+} and a Gd^{3+} ion in the same $\eta^1{:}\eta^1{:}\eta^2{:}\mu$ fashion (Scheme 2). In addition, the four triply-deprotonated $pypt^{3-}$ ligands bridge five metal ions, two Cu^{2+} and three Gd^{3+} ions, possessing the $\eta^1{:}\eta^2{:}\eta^2{:}\eta^2{:}\mu_5$ coordination mode. The coordination sphere of the Gd^{3+} ions is completed by 8 chelating NO_3^- ions (each Gd^{3+} ion is bound to two NO_3^- ions). Cu1 (and Cu1′) is four-coordinate, exhibiting a distorted square planar geometry. The *cis*- and *trans*-angles fall within the ranges of 86.0–96.3° and 161.6–165.5°, respectively, deviating slightly from the ideal 90° and 180° angles of a perfect square plane. Cu2 (and its symmetry equivalents) is five-coordinate, possessing a $\{CuO_3N_2\}$ coordination sphere. Employing the methodology proposed by Reedijk and Addison,[70] a trigonality index (τ) of 0.02 was determined, suggesting a distorted square pyramidal geometry (where τ is 0 and 1 for perfect square pyramidal and trigonal bipyramidal geometries, respectively). The axial Cu2–O5 bond length of 2.391 Å is notably longer than the bond lengths found in the basal plane, which range from 1.923 to 2.018 Å. The crystallographically unique Gd^{3+} ion is 8-coordinate with its coordination sphere being $\{GdO_8\}$. Its coordination geometry was estimated as distorted triangular dodecahedral, using the SHAPE 2.1 [71] program (Table S2†). There are no significant intermolecular interactions between neighboring clusters in the crystal structure of **1**·3MeCN, while the closest intermolecular metal···metal separation is 7.541 Å between Gd1 and Cu2 atoms of adjacent $[Cu_6Gd_4]$ complexes. To the best of our knowledge complex **1** is the first example of a $[Cu_6Gd_4]$ cluster and possesses an unprecedented metal/O core.

Magnetism studies

Static properties. Solid-state, variable-temperature direct current (dc) magnetic susceptibility measurements were performed on powdered polycrystalline samples of **1**–**4** in a 0.1 T field and in the 2.0–270 K range. The $\chi_M T$ *versus* T plots for all complexes are depicted in Fig. 2a (χ_M is the molar magnetic susceptibility). The experimental $\chi_M T$ values at 270 K (35.4 (**1**), 46.5 (**2**) and 57.1 (**3**) $cm^3\ mol^{-1}\ K$) are comparable to the expected ones (33.75 (**1**), 49.53 (**2**) and 58.93 (**3**) $cm^3\ mol^{-1}\ K$) for six Cu^{2+} ($S = 1/2$, $g = 2.0$) and four Gd^{3+} ($^8S_{7/2}$, $S = 7/2$, $L = 0$,

This journal is © The Royal Society of Chemistry 2024

Open Access Article. Published on 10 September 2024. Downloaded on 6/5/2026 2:59:47 PM.
This article is licensed under a Creative Commons Attribution-NonCommercial 3.0 Unported Licence.

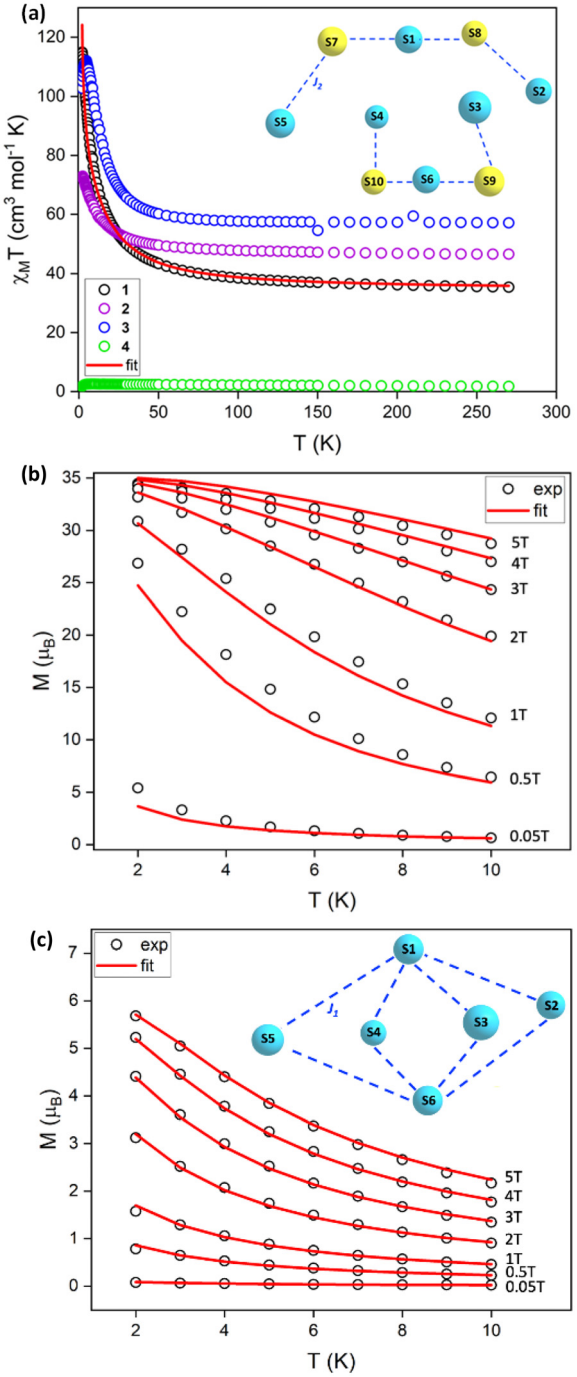

Fig. 2 (a) Temperature dependence of the $\chi_M T$ product for complexes **1–4** in a field of 0.1 T, (b) plot of the magnetization *versus* temperature data for **1**, (c) plot of the magnetization *versus* temperature data for **4**. Inset of 2a and 2c: representations of the isotropic exchange interactions included in spin-Hamiltonians used in the fit of the susceptibility and magnetization data for complexes **1** (a) and **4** (c). The red lines are a fit of the experimental data as described in the text.

g = 2.0) or Tb^{3+} ($^7F_6$, S = 3, L = 3, g = 3/2) or Dy^{3+} ($^6H_{15/2}$, S = 5/2, L = 5, g = 4/3) non-interacting ions.[72] The $\chi_M T$ product slightly increases upon cooling in all compounds to a value of 38.48 (**1**), 47.76 (**2**), and 57.64 (**3**) cm^3 mol^{-1} K at 100 K. Below this temperature, $\chi_M T$ increases more rapidly to a maximum value of 114.90 (**1**), 72.54 (**2**) cm^3 mol^{-1} K at 2 K, and 111.04 (**3**) cm^3 mol^{-1} K at 4.2 K. For **3**, the $\chi_M T$ product, after reaching this peak, decreases to 102.74 cm^3 mol^{-1} K at 2.0 K. The large increase in $\chi_M T$ values at low temperatures suggests the presence of dominant ferromagnetic interactions, with large spin ground states for all complexes while the slight decrease below 4.0 K observed for **3** could be attributed to the depopulation of the m$_j$ sublevels of the ground J state of the Dy^{3+} ions (Stark sublevels) and/or to weak antiferromagnetic interactions between the metal ions. For **4**, the $\chi_M T$ product increases from 1.78 cm^3 mol^{-1} K at 270 K to 2.55 cm^3 mol^{-1} K at 6.5 K and then decreases to 1.74 cm^3 mol^{-1} K at 2.0 K. The value at 270 K is smaller than the spin-only (g = 2.0) value of 2.25 cm^3 mol^{-1} K for six Cu^{2+} (S = 1/2) non-interacting ions.

Magnetization (M) studies were conducted for complexes **1–4**, under various low temperatures and magnetic fields (Fig. 2b, c and S4, S5†). The data for compound **1** reveal a rapid increase of the magnetization values with increase of the magnetic field, leading to a magnetization saturation at a value of ~34μ_B. This behaviour suggests the existence of a large spin ground state value, possibly S = 17 (assuming $g \approx 2$) which is the maximum S value for a [$Gd^{3+}{}_4Cu^{2+}{}_6$] compound. This indicates the presence of entirely ferromagnetic exchange interactions between the metal ions in **1**.

In contrast, the magnetization plots for **2** and **3** at 2.0 K exhibit a rapid increase up to 0.1 T, followed by a gradual, increase up to 22.76μ_B and 26.24μ_B at 5 T, respectively, without reaching saturation. The lack of saturation in magnetization of **2** and **3** is indicative of the presence of anisotropy. For **4**, M increases rapidly with increasing H at 2 K to the value of 5.68μ_B at 5 T without reaching saturation.

The magnetic susceptibility data for compounds **4** and **1** were fit to evaluate the strength of the intramolecular Cu^{2+}–Cu^{2+} and Cu^{2+}–Gd^{3+} magnetic exchange interactions, respectively. For complex **4**, the spin Hamiltonian used is shown below:

$$\hat{H}_1 = -2J_1 \sum_{i=1,6} \sum_{j=2}^{5} \hat{S}_i \hat{S}_j + \sum_{i=1}^{6} \mu_B B g_i \hat{S}_i$$

where the indices refer to the constituent Cu^{2+} ions, $\hat{S}$ is a spin operator and J_1 is the pairwise isotropic exchange interaction. For simplicity, we assume all magnetic exchange interactions between Cu^{2+}–Cu^{2+} ions to be equivalent (Fig. 2c, inset) and neglect anisotropy terms in the spin-Hamiltonian. In addition, considering that the exchange interactions between Cu^{2+} ions are expected to be very weak due to the magnetic coupling occurring *via* polyatomic bridges or simply through space, only the low-temperature magnetization data were fitted. This resulted in the best-fit parameter J_1 = −0.20 cm^{-1} (g = 2.0) indicating weak antiferromagnetic Cu^{2+}–Cu^{2+} exchange.

The $\chi_M T$ and magnetization data for complex **1** were simultaneously fit to the following spin-Hamiltonian:

$$\hat{H}_2 = -2J_2 \sum_{i,j} \hat{S}_i \hat{S}_j + \sum_{i=7}^{10} D_i \left[\hat{S}_{i,z}^2 - \frac{\hat{S}_i(\hat{S}_i + 1)}{3} \right] + \sum_{i=1}^{10} \mu_B B g_i \hat{S}_i$$

Open Access Article. Published on 10 September 2024. Downloaded on 6/5/2026 2:59:47 PM.
This article is licensed under a Creative Commons Attribution-NonCommercial 3.0 Unported Licence.

where the summation indices i, j run through the constitutive metal centres, D is the uniaxial single-ion anisotropy parameter for Gd^{3+} ions, $\hat{S}$ is a spin operator and J_2 is the isotropic Cu^{2+}–Gd^{3+} exchange interaction parameter. To avoid overparameterization, we assumed all magnetic exchange interactions between Cu^{2+}–Gd^{3+} ions to be equivalent (Fig. 2a, inset) and neglected Cu^{2+}–Cu^{2+} interactions. The best-fit parameters were J_2 = +4 cm^{-1} and $|D_{Gd}|$ = 6.5 × 10^{-3} cm^{-1} (g = 2.0). Including the Cu^{2+}–Cu^{2+} interactions in the model resulted in values similar to those determined in the case of **4** but did not significantly modify the quality of the fit. Thus, **1** can be described as containing ferromagnetic Cu^{2+}–Gd^{3+} interactions and consisting of two $\{Cu_3Gd_2\}$ pentametallic units, each with an S = 17/2 spin value, with the m_S = 17 projection being the ground state in the presence of a magnetic field. The reported J-coupling constant of **1** is in agreement with J_{ij} values reported for other Cu/Gd compounds.[29]

Dynamic properties. Alternating current (ac) magnetic susceptibility measurements were also performed to probe the magnetic dynamics of **1–3**, using a 3.5 Oe ac field. Complexes **2** and **3** show ac signals either in the absence or presence of an applied dc field. However, no peak maxima were observed in both cases suggesting fast magnetic relaxation most likely through quantum tunnelling of magnetization (QTM) (Fig. S7–S9†). Notably, complex **1**, containing isotropic Gd^{3+} ions, exhibits in-phase (χ') and out-of-phase (χ'') ac susceptibility signals under an applied dc field of 0.2 T (Fig. 3 and S6, S10†). Specifically, at frequencies below 60 Hz and temperatures below 5.3 K, complex **1** shows frequency dependent out-of-phase signals, indicative of magnetization relaxation at this time – scale. However, it was not possible to fit the experimental data and calculate the relaxation parameters since no peak maxima of the χ'' signals were observed in the frequency range of 1–1488 Hz from 1.8 to 5.3 K. In addition, attempts to fit the data using Kramers–Kronig relations[73,74] failed to produce reasonable values.

Notably, compound **1** which is based on an isotropic lanthanide ion displays out-of-phase signals at higher temperatures than the corresponding analogues (**2** and **3**) based on anisotropic ions. This could be attributed to the existence of different relaxation mechanisms in these compounds; strong quantum tunnelling dominates in anisotropic Tb and Dy complexes, whereas in Gd complex relaxation does not occur *via* the Orbach process but involves other mechanisms related to spin-phonon interactions. This behaviour has been observed recently in other compounds containing Gd^{3+} ions.[75–79]

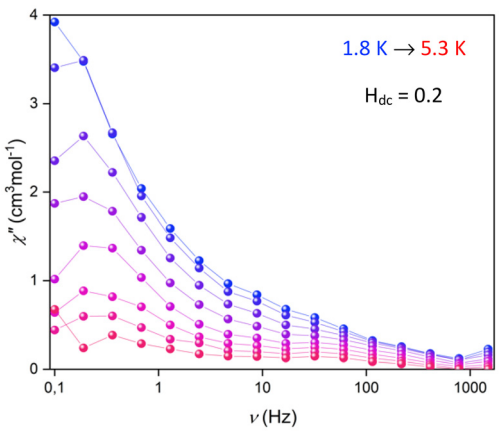

Fig. 3 Plot of the out-of-phase (χ''_M) signals *vs.* frequency (ν) for complex **1** under an applied dc field of 0.2 T.

Conclusions

The synthesis, crystal structures and magnetic studies of a new family of decanuclear $[Cu^{2+}{}_6M^{3+}{}_4]$ complexes [M = Gd (**1**), Tb (**2**), Dy (**3**), and Y (**4**)] are reported. These complexes were successfully synthesized from the initial employment of 2-(2-pyridyl)-1,3-propane-diol ($pypdH_2$) and 2-hydroxymethyl-2-(2-pyridyl)-1,3-propane-diol ($pyptH_3$) organic ligands. Complexes **1–4** feature a new metal stoichiometry and an unprecedented three-layered symmetric $[Cu_6M_4(\mu\text{-}OR)_{16}]^{8+}$ structural core. Dc magnetic susceptibility studies revealed the presence of ferromagnetic interactions and large spin ground state values, possibly S = 17 for the case of **1**. Ac studies revealed the presence of slow magnetic relaxation processes for all compounds. Work in progress includes the extension of the use of $pypdH_2$ and $pyptH_3$ ligands in 3d and/or 3d/4f cluster chemistry.

Experimental section

Materials, physical and spectroscopic measurements

Elemental analyses (C, H, and N) were performed by the in-house facilities of the University of Cyprus, Chemistry Department. IR spectra were recorded as ATR in the 4000–400 cm^{-1} range using a Shimadzu Prestige – 21 spectrometer. Variable-temperature dc and ac magnetic susceptibility data were collected at the University of Copenhagen using a Quantum Design MPMS-XL SQUID magnetometer equipped with a 7 T magnet and capable of operating in the 1.8–400 K range. Prior to measurements crystalline samples were crushed to microcrystalline powders and fixed in *n*-hexadecane to avoid orientation of the sample in the magnetic field. The ac magnetic susceptibility measurements were performed in an ac field of 3.5 G and in the presence or absence of an applied dc field. The oscillation frequencies were in the 0.1–1488 Hz range. Pascal's constants[80] were used to estimate the diamagnetic corrections, which were subtracted from the experimental susceptibilities to give the molar paramagnetic susceptibility (χ_M). The program PHI[81] was used to fit the magnetic data.

X-ray crystallography

Data were collected on a Rigaku XtaLAB Synergy-S single crystal X-ray diffractometer equipped with a CCD area detector and a graphite monochromator utilizing Cu Kα radiation (λ = 1.54184 Å). Selected crystals were attached to glass fiber with

This journal is © The Royal Society of Chemistry 2024

Open Access Article. Published on 10 September 2024. Downloaded on 6/5/2026 2:59:47 PM. This article is licensed under a Creative Commons Attribution-NonCommercial 3.0 Unported Licence.

paratone-N oil and transferred to a goniostat for data collection. Empirical absorption corrections (multiscan based on symmetry-related measurements) were applied using CrysAlis RED software.[82] The structures were solved by direct methods using SIR92[83] and refined on F^2 using SHELXL97,[84] SHELXL-2014/7,[85] and SHELXT.[86] Software packages used: CrysAlisCCD[82] for data collection, CrysAlisRED[82] for cell refinement and data reduction, WINGX for geometric calculations,[87] while MERCURY[88] and Diamond[89] were used for molecular graphics.

For all compounds, the non-H atoms were treated anisotropically, whereas the H atoms were placed in calculated, ideal positions and refined as riding on their respective C atoms. Unit cell parameters and structure solution and refinement data for complexes **1**·3MeCN, **2**·3MeCN, **3**·4MeCN and **4**·4MeCN are listed in Table S1 of the ESI.†

Syntheses

All manipulations were performed under aerobic conditions using materials (reagent grade) and solvents as received. The ligands 2-(2-pyridyl)-1,3-propane-diol ($pypdH_2$) and 2-hydroxymethyl-2-(2-pyridyl)-1,3-propane-diol ($pyptH_3$) were prepared, purified, and characterized as described elsewhere.[90] **Caution:** Although no such behaviour was observed during the present work, nitrate salts are potentially explosive; they should be synthesized and used in small quantities and treated with care.

$[Cu_6M_4(pypt)_4(pypdH)_4(NO_3)_8]$ [M = Gd (1), Tb (2), Dy (3), and Y (4)]. To a stirred, colourless solution of $pypdH_2$ (0.030 g, 0.2 mmol), $pyptH_3$ (0.040 g, 0.2 mmol) and NEt_3 (0.070 mL, 0.5 mmol) in MeCN/MeOH (2 : 1, 15 mL) were subsequently added solids $M(NO_3)_3{\cdot}xH_2O$ (x = 5 or 6) (0.2 mmol) and $Cu(NO_3)_2{\cdot}5/2H_2O$ (0.046 g, 0.2 mmol). The resulting blue solution was stirred for 30 min under mild heating (at ~50 °C). Then, the solution was filtered off, and the filtrate was left undisturbed at room temperature. After 1 day, dark blue block – shaped crystals of **1**·3MeCN, **2**·3MeCN, **3**·4MeCN and **4**·4MeCN appeared, which were kept in mother liquor for X-ray analysis, or collected by filtration, washed with MeCN, and dried in air for other solid-state studies. The reaction yields were in the range of ~45–65%. Anal. Calc. (found); $C_{68}H_{100}N_{16}O_{54}Cu_6Gd_4$ (**1**·10H_2O): C, 27.08 (27.32); H, 3.34 (3.52); N, 7.43 (7.67)%; $C_{68}H_{108}N_{16}O_{58}Cu_6Tb_4$ (**2**·14H_2O): C, 26.39 (26.67); H, 3.52 (3.73); N, 7.24 (7.58)%; $C_{68}H_{110}N_{16}O_{59}Cu_6Dy_4$ (**3**·15H_2O): C, 26.12 (26.31); H, 3.55 (3.51); N, 7.17 (7.38)%; $C_{68}H_{100}N_{16}O_{54}Cu_6Y_4$ (**4**·10H_2O): C, 29.78 (29.69); H, 3.68 (3.53); N, 8.17 (7.98)%.

Data availability

The data supporting this article (various structural tables, spectroscopic and magnetic figures and tables for complexes **1–4**) have been included as part of the ESI.†

Crystallographic data for **1**·3MeCN, **2**·3MeCN, **3**·4MeCN and **4**·4MeCN has been deposited at the CCDC under 2370731–2370734† numbers and can be obtained from **https://www.ccdc.cam.ac.uk/structures/**.

Conflicts of interest

There are no conflicts to declare.

Acknowledgements

This work was supported by the Cyprus Research and Innovation Foundation Research Grant "EXCELLENCE/0421/0399" which is co-funded by the Republic of Cyprus and the European Regional Development Fund.

References

1 C.-M. Liu, S.-D. Zhu, Y.-B. Lu, X. Hao and H.-R. Wen, Homochiral Cu_6Dy_3 single-molecule magnets displaying proton conduction and a strong magneto-optical Faraday effect, *Inorg. Chem. Front.*, 2023, **10**, 3714–3722.

2 A. Bhanja, S. Roy Chaudhuri, A. B. Canaj, S. P. Vyas, F. Ortu, L. Smythe, M. Murrie, R. Goswami and D. Ray, Synthesis and characterization of two self-assembled $[Cu_6Gd_3]$ and $[Cu_5Dy_2]$ complexes exhibiting the magnetocaloric effect, slow relaxation of magnetization, and anticancer activity, *Dalton Trans.*, 2023, **52**, 3795–3806.

3 J. Wang, Q.-W. Li, S.-G. Wu, Y.-C. Chen, R.-C. Wan, G.-Z. Huang, Y. Liu, J.-L. Liu, D. Reta, M. J. Giansiracusa, *et al.*, Opening Magnetic Hysteresis by Axial Ferromagnetic Coupling: From Mono-Decker to Double-Decker Metallacrown, *Angew. Chem., Int. Ed.*, 2021, **60**, 5299–5306.

4 A. Bencini, C. Benelli, A. Caneschi, A. Dei and D. Gatteschi, Crystal and molecular structure and magnetic properties of a trinuclear complex containing exchange-coupled $GdCu_2$ species, *Inorg. Chem.*, 1986, **25**, 572–575.

5 S. Osa, T. Kido, N. Matsumoto, N. Re, A. Pochaba and J. Mrozinski, A Tetranuclear 3d–4f Single Molecule Magnet: $[CuIILTbIII(hfac)_2]_2$, *J. Am. Chem. Soc.*, 2004, **126**, 420–421.

6 J.-D. Leng, J.-L. Liu and M.-L. Tong, Unique nanoscale $\{CuII_{36}LnIII_{24}\}$ (Ln = Dy and Gd) metallo-rings, *Chem. Commun.*, 2012, **48**, 5286–5288.

7 V. Baskar, K. Gopal, M. Helliwell, F. Tuna, W. Wernsdorfer and R. E. P. Winpenny, 3d–4f Clusters with large spin ground states and SMM behaviour, *Dalton Trans.*, 2010, **39**, 4747–4750.

8 S. Yu, H. Hu, Z. Qiu, Y. Zhang, D. Liu, Y. Liang, H.-H. Zou, F.-P. Liang and Z. Chen, Structure and assembly mechanism of a centipede-shaped high-nuclear $Dy_{14}Cu_{12}$ heterometallic nanocluster, *CrystEngComm*, 2023, **25**, 114–121.

9 X. Xu, Y. He, W. Meng, L. Yao, L. Liu, C. Zhao and F. Xu, Chiral wheel anions of copper(II)-early lanthanides(iii) with high optical-limiting properties, *Dalton Trans.*, 2022, **51**, 5414–5418.

Open Access Article. Published on 10 September 2024. Downloaded on 6/5/2026 2:59:47 PM. This article is licensed under a Creative Commons Attribution-NonCommercial 3.0 Unported Licence.

10 S. Xiang, S. Hu, T. Sheng, R. Fu, X. Wu and X. Zhang, A Fan-Shaped Polynuclear Gd_6Cu_{12} Amino Acid Cluster:A "Hollow" and Ferromagnetic $[Gd_6(\mu_3\text{-}OH)_8]$ Octahedral Core Encapsulated by Six $[Cu_2]$ Glycinato Blade Fragments, *J. Am. Chem. Soc.*, 2007, **129**, 15144–15146.

11 J.-L. Liu, Y.-C. Chen, Q.-W. Li, S. Gómez-Coca, D. Aravena, E. Ruiz, W.-Q. Lin, J.-D. Leng and M.-L. Tong, Two 3d–4f nanomagnets formed via a two-step in situ reaction of picolinaldehyde, *Chem. Commun.*, 2013, **49**, 6549–6551.

12 Y. Xing, L.-Q. Chen, Y.-R. Zhao, X.-Y. Zheng, Y.-J. Zhang, X.-J. Kong, L.-S. Long and L.-S. Zheng, High-Nuclearity Chiral 3d-4f Heterometallic Clusters Ln_6Cu_{24} and Ln_6Cu_{12}, *Inorg. Chem.*, 2019, **58**, 8494–8499.

13 I. A. Kühne, K. Griffiths, A.-J. Hutchings, O. P. E. Townrow, A. Eichhöfer, C. E. Anson, G. E. Kostakis and A. K. Powell, Stepwise Investigation of the Influences of Steric Groups versus Counterions to Target Cu/Dy Complexes, *Cryst. Growth Des.*, 2017, **17**, 5178–5190.

14 P. Kumar, K. Griffiths, C. E. Anson, A. K. Powell and G. E. Kostakis, A tetranuclear $CuII_2DyIII_2$ coordination cluster as a Suzuki (C–C) coupling reaction promoter, *Dalton Trans.*, 2018, **47**, 17202–17205.

15 R. Bagai and G. Christou, The Drosophila of single-molecule magnetism: $[Mn_{12}O_{12}(O_2CR)_{16}(H_2O)_4]$, *Chem. Soc. Rev.*, 2009, **38**, 1011–1026.

16 A. Zabala-Lekuona, J. M. Seco and E. Colacio, Single-Molecule Magnets: From Mn_{12}-ac to dysprosium metallocenes, a travel in time, *Coord. Chem. Rev.*, 2021, **441**, 213984.

17 E. Coronado, Molecular magnetism: from chemical design to spin control in molecules, materials and devices, *Nat. Rev. Mater.*, 2020, **5**, 87–104.

18 M. Evangelisti and E. K. Brechin, Recipes for enhanced molecular cooling, *Dalton Trans.*, 2010, **39**, 4672–4676.

19 J.-L. Liu, Y.-C. Chen, F.-S. Guo and M.-L. Tong, Recent advances in the design of magnetic molecules for use as cryogenic magnetic coolants, *Coord. Chem. Rev.*, 2014, **281**, 26–49.

20 R. Sessoli and A. K. Powell, Strategies towards single molecule magnets based on lanthanide ions, *Coord. Chem. Rev.*, 2009, **253**, 2328–2341.

21 J. D. Rinehart and J. R. Long, Exploiting single-ion anisotropy in the design of f-element single-molecule magnets, *Chem. Sci.*, 2011, **2**, 2078–2085.

22 R. Marin, G. Brunet and M. Murugesu, Shining New Light on Multifunctional Lanthanide Single-Molecule Magnets, *Angew. Chem., Int. Ed.*, 2021, **60**, 1728–1746.

23 J.-L. Liu, Y.-C. Chen and M.-L. Tong, Symmetry strategies for high performance lanthanide-based single-molecule magnets, *Chem. Soc. Rev.*, 2018, **47**, 2431–2453.

24 N. Ishikawa, M. Sugita and W. Wernsdorfer, Quantum Tunneling of Magnetization in Lanthanide Single-Molecule Magnets: Bis(phthalocyaninato)terbium and Bis(phthalocyaninato)dysprosium Anions, *Angew. Chem., Int. Ed.*, 2005, **44**, 2931–2935.

25 C. Benelli, A. Caneschi, D. Gatteschi, O. Guillou and L. Pardi, Synthesis, crystal structure, and magnetic properties of tetranuclear complexes containing exchange-coupled dilanthanide-dicopper(lanthanide = gadolinium, dysprosium) species, *Inorg. Chem.*, 1990, **29**, 1750–1755.

26 M. Andruh, I. Ramade, E. Codjovi, O. Guillou, O. Kahn and J. C. Trombe, Crystal structure and magnetic properties of $[Ln_2Cu_4]$ hexanuclear clusters (where Ln = trivalent lanthanide). Mechanism of the gadolinium(III)-copper(II) magnetic interaction, *J. Am. Chem. Soc.*, 1993, **115**, 1822–1829.

27 N. Ahmed, T. Sharma, L. Spillecke, C. Koo, K. U. Ansari, S. Tripathi, A. Caneschi, R. Klingeler, G. Rajaraman and M. Shanmugam, Probing the Origin of Ferro-/Antiferromagnetic Exchange Interactions in Cu(II)–4f Complexes, *Inorg. Chem.*, 2022, **61**, 5572–5587.

28 A. Panja, S. Paul, E. Moreno-Pineda, R. Herchel, N. C. Jana, P. Brandão, G. Novitchi and W. Wernsdorfer, Insight into ferromagnetic interactions in CuII–LnIII dimers with a compartmental ligand, *Dalton Trans.*, 2024, **53**, 2501–2511.

29 A. Dey, P. Bag, P. Kalita and V. Chandrasekhar, Heterometallic CuII–LnIII complexes: Single molecule magnets and magnetic refrigerants, *Coord. Chem. Rev.*, 2021, **432**, 213707.

30 S. K. Langley, L. Ungur, N. F. Chilton, B. Moubaraki, L. F. Chibotaru and K. S. Murray, Structure, Magnetism and Theory of a Family of Nonanuclear $CuII_5LnIII_4$-Triethanolamine Clusters Displaying Single-Molecule Magnet Behaviour, *Chem. – Eur. J.*, 2011, **17**, 9209–9218.

31 H. L. C. Feltham, R. Clérac, L. Ungur, L. F. Chibotaru, A. K. Powell and S. Brooker, By Design: A Macrocyclic 3d–4f Single-Molecule Magnet with Quantifiable Zero-Field Slow Relaxation of Magnetization, *Inorg. Chem.*, 2013, **52**, 3236–3240.

32 J. Wu, L. Zhao, L. Zhang, X.-L. Li, M. Guo, A. K. Powell and J. Tang, Macroscopic Hexagonal Tubes of 3d–4f Metallocycles, *Angew. Chem., Int. Ed.*, 2016, **55**, 15574–15578.

33 M. J. H. Ojea, V. A. Milway, G. Velmurugan, L. H. Thomas, S. J. Coles, C. Wilson, W. Wernsdorfer, G. Rajaraman and M. Murrie, Enhancement of TbIII–CuII Single-Molecule Magnet Performance through Structural Modification, *Chem. – Eur. J.*, 2016, **22**, 12839–12848.

34 L. R. Piquer and E. C. Sañudo, Heterometallic 3d–4f single-molecule magnets, *Dalton Trans.*, 2015, **44**, 8771–8780.

35 T. N. Hooper, J. Schnack, S. Piligkos, M. Evangelisti and E. K. Brechin, The Importance of Being Exchanged: $[GdIII_4MII_8(OH)_8(L)_8(O_2CR)_8]^{4+}$ Clusters for Magnetic Refrigeration, *Angew. Chem., Int. Ed.*, 2012, **51**, 4633–4636.

36 S. K. Langley, B. Moubaraki, C. Tomasi, M. Evangelisti, E. K. Brechin and K. S. Murray, Synthesis, Structure, and Magnetism of a Family of Heterometallic $\{Cu_2Ln_7\}$ and $\{Cu_4Ln_{12}\}$ (Ln = Gd, Tb, and Dy) Complexes: The Gd Analogues Exhibiting a Large Magnetocaloric Effect, *Inorg. Chem.*, 2014, **53**, 13154–13161.

37 E. M. Pineda, C. Heesing, F. Tuna, Y.-Z. Zheng, E. J. L. McInnes, J. Schnack and R. E. P. Winpenny, Copper

 This journal is © The Royal Society of Chemistry 2024

Open Access Article. Published on 10 September 2024. Downloaded on 6/5/2026 2:59:47 PM. This article is licensed under a Creative Commons Attribution-NonCommercial 3.0 Unported Licence.

Lanthanide Phosphonate Cages: Highly Symmetric $\{Cu_3Ln_9P_6\}$ and $\{Cu_6Ln_6P_6\}$ Clusters with C_{3v} and D_{3h} Symmetry, *Inorg. Chem.*, 2015, **54**, 6331–6337.

38 D. I. Alexandropoulos, K. M. Poole, L. Cunha-Silva, J. A. Sheikh, W. Wernsdorfer, G. Christou and T. C. Stamatatos, A family of 'windmill'-like $\{Cu_6Ln_{12}\}$ complexes exhibiting single-molecule magnetism behavior and large magnetic entropy changes, *Chem. Commun.*, 2017, **53**, 4266–4269.

39 Y.-Z. Zheng, M. Evangelisti and R. E. P. Winpenny, Co–Gd phosphonate complexes as magnetic refrigerants, *Chem. Sci.*, 2011, **2**, 99–102.

40 D. Dermitzaki, V. Psycharis, Y. Sanakis, T. C. Stamatatos, M. Pissas and C. P. Raptopoulou, Extending the family of heptanuclear heterometallic Cu_5Ln_2 (Ln = Gd, Tb, Dy) complexes: Synthesis, crystal structures, magnetic and magnetocaloric studies, *Polyhedron*, 2019, **169**, 135–143.

41 K. Liu, W. Shi and P. Cheng, Toward heterometallic single-molecule magnets: Synthetic strategy, structures and properties of 3d–4f discrete complexes, *Coord. Chem. Rev.*, 2015, **289–290**, 74–122.

42 A. Worrell, D. Sun, J. Mayans, C. Lampropoulos, A. Escuer and T. C. Stamatatos, Oximato-Based Ligands in 3d/4f-Metal Cluster Chemistry: A Family of $\{Cu_3Ln\}$ Complexes with a "Propeller"-like Topology and Single-Molecule Magnetic Behavior, *Inorg. Chem.*, 2018, **57**, 13944–13952.

43 P. Richardson, K. J. Gagnon, S. J. Teat, G. Lorusso, M. Evangelisti, J. Tang and T. C. Stamatatos, New Dioximes as Bridging Ligands in 3d/4f-Metal Cluster Chemistry: One-Dimensional Chains of Ferromagnetically Coupled $\{Cu_6Ln_2\}$ Clusters Bearing Acenaphthenequinone Dioxime and Exhibiting Magnetocaloric Properties, *Cryst. Growth Des.*, 2017, **17**, 2486–2497.

44 D. Dermitzaki, G. Lorusso, C. P. Raptopoulou, V. Psycharis, A. Escuer, M. Evangelisti, S. P. Perlepes and T. C. Stamatatos, Molecular Nanoscale Magnetic Refrigerants: A Ferrimagnetic $\{CuII_{15}GdIII_7\}$ Cagelike Cluster from the Use of Pyridine-2,6-dimethanol, *Inorg. Chem.*, 2013, **52**, 10235–10237.

45 P. Richardson, D. I. Alexandropoulos, L. Cunha-Silva, G. Lorusso, M. Evangelisti, J. Tang and T. C. Stamatatos, 'All three-in-one': ferromagnetic interactions, single-molecule magnetism and magnetocaloric properties in a new family of $[Cu_4Ln]$ (LnIII = Gd, Tb, Dy) clusters, *Inorg. Chem. Front.*, 2015, **2**, 945–948.

46 D. I. Alexandropoulos, L. Cunha-Silva, J. Tang and T. C. Stamatatos, Heterometallic Cu/Ln cluster chemistry: ferromagnetically-coupled $\{Cu_4Ln_2\}$ complexes exhibiting single-molecule magnetism and magnetocaloric properties, *Dalton Trans.*, 2018, **47**, 11934–11941.

47 D. Dermitzaki, C. P. Raptopoulou, V. Psycharis, A. Escuer, S. P. Perlepes, J. Mayans and T. C. Stamatatos, Further synthetic investigation of the general lanthanoid(iii) [Ln(iii)]/copper(II)/pyridine-2,6-dimethanol/carboxylate reaction system: $\{CuII_5LnIII_4\}$ coordination clusters (Ln = Dy, Tb, Ho) and their yttrium(III) analogue, *Dalton Trans.*, 2021, **50**, 240–251.

48 J.-J. Zhang, T.-L. Sheng, S.-Q. Xia, G. Leibeling, F. Meyer, S.-M. Hu, R.-B. Fu, S.-C. Xiang and X.-T. Wu, Syntheses and Characterizations of a Series of Novel Ln_6Cu_{24} Clusters with Amino Acids as Ligands, *Inorg. Chem.*, 2004, **43**, 5472–5478.

49 G. J. Sopasis, A. B. Canaj, A. Philippidis, M. Siczek, T. Lis, J. R. O'Brien, M. M. Antonakis, S. A. Pergantis and C. J. Milios, Heptanuclear Heterometallic $[Cu_6Ln]$ Clusters: Trapping Lanthanides into Copper Cages with Artificial Amino Acids, *Inorg. Chem.*, 2012, **51**, 5911–5918.

50 A. B. Canaj, D. I. Tzimopoulos, M. Otręba, T. Lis, R. Inglis and C. J. Milios, Solvothermal synthesis of enneanuclear $[CuII_7LnIII_2]$ clusters, *Dalton Trans.*, 2015, **44**, 19880–19885.

51 D. Maniaki, E. Pilichos and S. P. Perlepes, Coordination Clusters of 3d-Metals That Behave as Single-Molecule Magnets (SMMs): Synthetic Routes and Strategies, *Front. Chem.*, 2018, **6**, 461.

52 W. Lv, S.-D. Han, X.-Y. Li and G.-M. Wang, Coordination chemistry and magnetic properties of polynuclear metal clusters/cluster-based frameworks with tripodal alcohol ligands, *Coord. Chem. Rev.*, 2023, **495**, 215376.

53 S. Mukherjee, Y. P. Patil and P. S. Mukherjee, Two Novel Heterometallic Chains Featuring MnII and NaI Ions in Trigonal-Prismatic Geometries Alternately Linked to Octahedral MnIV Ions: Synthesis, Structures, and Magnetic Behavior, *Inorg. Chem.*, 2012, **51**, 4888–4890.

54 L. Yang, D. R. Powell and R. P. Houser, Copper(II) coordination chemistry of 2-methyl-2-(2-pyridyl)-1,3-propan-diol: Syntheses and structures of mono-, di-, and tricopper complexes, *Polyhedron*, 2010, **29**, 1946–1955.

55 E. E. Moushi, C. Lampropoulos, W. Wernsdorfer, V. Nastopoulos, G. Christou and A. J. Tasiopoulos, Inducing Single-Molecule Magnetism in a Family of Loop-of-Loops Aggregates: Heterometallic $Mn_{40}Na_4$ Clusters and the Homometallic Mn_{44} Analogue, *J. Am. Chem. Soc.*, 2010, **132**, 16146–16155.

56 M. Charalambous, E. E. Moushi, T. N. Nguyen, A. M. Mowson, G. Christou and A. J. Tasiopoulos, $[Mn_{14}]$ "Structural Analogues" of Well-Known $[Mn_{12}]$ Single-Molecule Magnets, *Eur. J. Inorg. Chem.*, 2018, **2018**, 3905–3912.

57 C. Papatriantafyllopoulou, S. Zartilas, M. J. Manos, C. Pichon, R. Clérac and A. J. Tasiopoulos, A single-chain magnet based on linear $[MnIII_2MnII]$ units, *Chem. Commun.*, 2014, **50**, 14873–14876.

58 S. Zartilas, C. Papatriantafyllopoulou, T. C. Stamatatos, V. Nastopoulos, E. Cremades, E. Ruiz, G. Christou, C. Lampropoulos and A. J. Tasiopoulos, A $MnII_6MnIII_6$ Single-Strand Molecular Wheel with a Reuleaux Triangular Topology: Synthesis, Structure, Magnetism, and DFT Studies, *Inorg. Chem.*, 2013, **52**, 12070–12079.

59 A. J. Tasiopoulos and S. P. Perlepes, Diol-type ligands as central 'players' in the chemistry of high-spin molecules

Open Access Article. Published on 10 September 2024. Downloaded on 6/5/2026 2:59:47 PM. This article is licensed under a Creative Commons Attribution-NonCommercial 3.0 Unported Licence.

and single-molecule magnets, *Dalton Trans.*, 2008, **41**, 5537–5555.

60 E. K. Brechin, Using tripodal alcohols to build high-spin molecules and single-molecule magnets, *Chem. Commun.*, 2005, **41**, 5141–5153.

61 M. Manoli, R. Inglis, M. J. Manos, V. Nastopoulos, W. Wernsdorfer, E. K. Brechin and A. J. Tasiopoulos, A [Mn_{32}] Double-Decker Wheel, *Angew. Chem., Int. Ed.*, 2011, **50**, 4441, ·3MeCN, 2·3MeCN, 3·4MeCN and 4·4MeCN 444.

62 M. Manoli, R. Inglis, M. J. Manos, G. S. Papaefstathiou, E. K. Brechin and A. J. Tasiopoulos, A 1-D coordination polymer based on a Mn_{40} octagonal super-structure, *Chem. Commun.*, 2013, **49**, 1061–1063.

63 M. Manoli, R. Inglis, S. Piligkos, Y. Li, W. Wernsdorfer, E. K. Brechin and A. J. Tasiopoulos, A hexameric [$MnIII_{18}Na_6$] wheel based on $[MnIII_3O]^{7+}$ sub-units, *Chem. Commun.*, 2016, **52**, 12829–12832.

64 M. Savva, K. Skordi, A. D. Fournet, A. E. Thuijs, G. Christou, S. P. Perlepes, C. Papatriantafyllopoulou and A. J. Tasiopoulos, Heterometallic $MnIII_4Ln_2$ (Ln = Dy, Gd, Tb) Cross-Shaped Clusters and Their Homometallic $MnIII_4MnII_2$ Analogues, *Inorg. Chem.*, 2017, **56**, 5657–5668.

65 K. Skordi, A. Anastassiades, A. D. Fournet, R. Kumar, M. Schulze, W. Wernsdorfer, G. Christou, V. Nastopoulos, S. P. Perlepes, C. Papatriantafyllopoulou, *et al.*, High nuclearity structurally – related Mn supertetrahedral T_4 aggregates, *Chem. Commun.*, 2021, **57**, 12484–12487.

66 K. Skordi, D. I. Alexandropoulos, A. D. Fournet, N. Panagiotou, E. E. Moushi, C. Papatriantafyllopoulou, G. Christou and A. J. Tasiopoulos, Rare Nuclearities and Unprecedented Structural Motifs in Manganese Cluster Chemistry from the Combined Use of Di-2-Pyridyl Ketone with Selected Diols, *Chemistry*, 2023, **5**, 1681–1695.

67 K. Skordi, D. I. Alexandropoulos, A. D. Fournet, N. Panagiotou, S. P. Perlepes, G. Christou and A. J. Tasiopoulos, Mixed-Valence Manganese Carboxylate Clusters, {$MnIII_6MnII_4$}, {$MnIII_7MnII_5Na$}, and {$MnIII_7MnII_5$}, Derived from the Combined Use of Di-2-pyridyl Ketone with Selected Aliphatic Diols, *Eur. J. Inorg. Chem.*, 2024, e202300735.

68 W. Liu and H. H. Thorp, Bond valence sum analysis of metal-ligand bond lengths in metalloenzymes and model complexes. 2. Refined distances and other enzymes, *Inorg. Chem.*, 1993, **32**, 4102–4105.

69 I. D. Brown and D. Altermatt, Bond-valence parameters obtained from a systematic analysis of the Inorganic Crystal Structure Database, *Acta Crystallogr., Sect. B: Struct. Sci.*, 1985, **41**, 244–247.

70 A. W. Addison, T. N. Rao, J. Reedijk, J. van Rijn and G. C. Verschoor, Synthesis, structure, and spectroscopic properties of copper(II) compounds containing nitrogen–sulphur donor ligands; the crystal and molecular structure of aqua[1,7-bis(N-methylbenzimidazol-2′-yl)-2,6-dithiaheptane]copper(II) perchlorate, *J. Chem. Soc., Dalton Trans.*, 1984, **7**, 1349–1356.

71 S. Alvarez, P. Alemany, D. Casanova, J. Cirera, M. Llunell and D. Avnir, Shape maps and polyhedral interconversion paths in transition metal chemistry, *Coord. Chem. Rev.*, 2005, **249**, 1693–1708.

72 C. Benelli and D. Gatteschi, Magnetism of Lanthanides in Molecular Materials with Transition-Metal Ions and Organic Radicals, *Chem. Rev.*, 2002, **102**, 2369–2388.

73 K. S. Cole and R. H. Cole, Dispersion and absorption in dielectrics I. Alternating current characteristics, *J. Chem. Phys.*, 1941, **9**, 341–351.

74 J. Bartolomé, G. Filoti, V. Kuncser, G. Schinteie, V. Mereacre, C. E. Anson, A. K. Powell, D. Prodius and C. Turta, Magnetostructural correlations in the tetranuclear series of butterfly core clusters: Magnetic and M"ossbauer spectroscopic study, *Phys. Rev. B: Condens. Matter Mater. Phys.*, 2009, **80**, 014430.

75 R. J. Holmberg, L. T. A. Ho, L. Ungur, I. Korobkov, L. F. Chibotaru and M. Murugesu, Observation of unusual slow-relaxation of the magnetisation in a Gd-EDTA chelate, *Dalton Trans.*, 2015, **44**, 20321–20325.

76 J. Mayans and A. Escuer, Correlating the axial Zero Field Splitting with the slow magnetic relaxation in GdIII SIMs, *Chem. Commun.*, 2021, **57**, 721–724.

77 I. Mylonas-Margaritis, Z. G. Lada, A. A. Kitos, D. Maniaki, K. Skordi, A. J. Tasiopoulos, V. Bekiari, A. Escuer, J. Mayans, V. Nastopoulos, *et al.*, Interesting chemical and physical features of the products of the reactions between trivalent lanthanoids and a tetradentate Schiff base derived from cyclohexane-1,2-diamine, *Dalton Trans.*, 2023, **52**, 8332–8343.

78 S. Caballero, E. Pilichos, M. Font-Bardia, J. Mayans and A. Escuer, Field-Induced Slow Magnetic Relaxation in a New Family of Tetranuclear Double-Stranded Cu_2II–Ln_2III Metallohelicates, *Cryst. Growth Des.*, 2023, **23**, 3711–3719.

79 B. Liu, B. Wang, Z. Wang and S. Gao, Static field induced magnetic relaxations in dinuclear lanthanide compounds of $[phen_2Ln_2(HCOO)_4(HCOO)_{2-2x}(NO_3)_{2x}]$ (1, Ln = Gd and x = 0.52; 2, Ln = Er and x = 0.90; phen = 1,10-phenanthroline), *Sci. China: Chem.*, 2012, **55**, 926–933.

80 G. A. Bain and J. F. Berry, Diamagnetic Corrections and Pascal's Constants, *J. Chem. Educ.*, 2008, **85**, 532.

81 N. F. Chilton, R. P. Anderson, L. D. Turner, A. Soncini and K. S. Murray, PHI: A powerful new program for the analysis of anisotropic monomeric and exchange-coupled polynuclear d- and f-block complexes, *J. Comput. Chem.*, 2013, **34**, 1164–1175.

82 P. Loeffen, *Oxford Diffraction., CrysAlis CCD and CrysAlis RED*, Oxford Diffraction Ltd., Abingdon, UK, 2008.

83 A. Altomare, G. Cascarano, C. Giacovazzo, A. Guagliardi, M. C. Burla, G. Polidori and M. Camalli, SIR92 - a program for automatic solution of crystal structures by direct methods, *J. Appl. Crystallogr.*, 1994, **27**, 435.

84 S. G. M. Shelxl, *Program for the Refinement of Crystal Structures*, University of Göttingen, Göttingen, Germany, 1997.

 This journal is © The Royal Society of Chemistry 2024

Open Access Article. Published on 10 September 2024. Downloaded on 6/5/2026 2:59:47 PM.
This article is licensed under a Creative Commons Attribution-NonCommercial 3.0 Unported Licence.

85 G. M. Sheldrick, *SHELXL-2014, Program for the refinement of crystal structures*, University of Göttingen, Germany, 2014.
86 D. Oxford, *CrysAlis CCD and CrysAlis RED, version 1.71*, Oxford Diffraction, Oxford, England, 2007.
87 L. J. Farrugia, WinGX suite for small-molecule single-crystal crystallography, *J. Appl. Crystallogr.*, 1999, **32**, 837–838.
88 C. F. Macrae, P. R. Edgington, P. McCabe, E. Pidcock, G. P. Shields, R. Taylor, M. Towler and J. V. D. Streek, Mercury: visualization and analysis of crystal structures, *J. Appl. Crystallogr.*, 2006, **39**, 453–457.
89 K. Brandenburg and H. Putz, *DIAMOND*, Crystal Impact GbR, Bonn, Germany, 2006.
90 W. F. Bailey, K. M. Lambert, Z. D. Stempel, K. B. Wiberg and B. Q. Mercado, Controlling the Conformational Energy of a Phenyl Group by Tuning the Strength of a Nonclassical CH···O Hydrogen Bond: The Case of 5-Phenyl-1,3-dioxane, *J. Org. Chem.*, 2016, **81**, 12116–12127.